

MICROCOPY RESOLUTION TEST CHART
NATIONAL BUREAU OF STANDARDS-1963-A

2

AFGL-TR-84-0236
AIR FORCE SURVEYS IN GEOPHYSICS, NO. 446

AD-A154 517

Global Geoid and Gravity Anomaly Predictions Using the Collocation and Point Mass Techniques

ROBERT P. BESSETTE
GEORGE HADGIGEORGE



6 September 1984



Approved for public release; distribution unlimited.



DTIC
ELECTE
JUN 5 1985
S D
E

DTIC FILE COPY



EARTH SCIENCES DIVISION

PROJECT 2309

AIR FORCE GEOPHYSICS LABORATORY

HANSCOM AFB, MA 01731

85 5 07 070

IN-HOUSE REPORTS

This technical report has been reviewed and is approved for publication.

FOR THE COMMANDER



THOMAS P. ROONEY
Chief, Geodesy & Gravity Branch



THOMAS P. ROONEY
Acting Director
Earth Sciences Division

This document has been reviewed by the FSD Public Affairs Office (PA) and is releasable to the National Technical Information Service (NTIS).

Qualified requestors may obtain additional copies from the Defense Technical Information Center. All others should apply to the National Technical Information Service.

If your address has changed, or if you wish to be removed from the mailing list, or if the addressee is no longer employed by your organization, please notify AFGL/DAA, Hanscom AFB, MA 01731. This will assist us in maintaining a current mailing list.

Unclassified

SECURITY CLASSIFICATION OF THIS PAGE

REPORT DOCUMENTATION PAGE					
1a. REPORT SECURITY CLASSIFICATION Unclassified		1b. RESTRICTIVE MARKINGS			
2a. SECURITY CLASSIFICATION AUTHORITY		3. DISTRIBUTION/AVAILABILITY OF REPORT Approved for public release; distribution unlimited.			
2b. DECLASSIFICATION/DOWNGRADING SCHEDULE					
4. PERFORMING ORGANIZATION REPORT NUMBER(S) AFGL-TR-84-0236 AFSG, No. 446		5. MONITORING ORGANIZATION REPORT NUMBER(S)			
6a. NAME OF PERFORMING ORGANIZATION Air Force Geophysics Laboratory	6b. OFFICE SYMBOL (If applicable) LWG	7a. NAME OF MONITORING ORGANIZATION			
6c. ADDRESS (City, State and ZIP Code) Hanscom AFB Massachusetts 01731		7b. ADDRESS (City, State and ZIP Code)			
8a. NAME OF FUNDING/SPONSORING ORGANIZATION	8b. OFFICE SYMBOL (If applicable)	9. PROCUREMENT INSTRUMENT IDENTIFICATION NUMBER			
8c. ADDRESS (City, State and ZIP Code)		10. SOURCE OF FUNDING NOS.			
		PROGRAM ELEMENT NO.	PROJECT NO.	TASK NO.	WORK UNIT NO.
11. TITLE (Include Security Classification) Global Geoid and Gravity Anomaly Predictions. (Contd)		61102F	2309	2309G1	2309G109
12. PERSONAL AUTHOR(S) Robert P. Bessette and George Hadgigeorge					
13a. TYPE OF REPORT Scientific Interim	13b. TIME COVERED FROM Jan 84 TO Aug 84	14. DATE OF REPORT (Yr., Mo., Day) 1984 September 6	15. PAGE COUNT 23		
16. SUPPLEMENTARY NOTATION					
17. COSATI CODES			18. SUBJECT TERMS (Continue on reverse if necessary and identify by block number)		
FIELD	GROUP	SUB GR	Altimetry Gravity Geoid		
19. ABSTRACT (Continue on reverse if necessary and identify by block number)					
<p>We previously described (14, 14) spherical-harmonic global adjustments of satellite altimetry using the AFGL short-arc technique supplemented with point masses to allow incorporation of short-wavelength geoidal detail. Recently, we have also investigated another technique to enhance short-wavelength detail; least squares collocation with noise. Both methods provide a means to determine a high resolution gravity field on a local, regional or global scale. Statistical comparisons of these two methods have been made in selected areas and the results tabulated.</p>					
20. DISTRIBUTION AVAILABILITY OF ABSTRACT UNCLASSIFIED/UNLIMITED <input checked="" type="checkbox"/> SAME AS RPT <input type="checkbox"/> DTIC USERS <input type="checkbox"/>			21. ABSTRACT SECURITY CLASSIFICATION Unclassified		
22a. NAME OF RESPONSIBLE INDIVIDUAL Robert P. Bessette		22b. TELEPHONE NUMBER (Include Area Code) (617) 861-3078	22c. OFFICE SYMBOL AFGL/LWG		

DD FORM 1473, 83 APR

EDITION OF 1 JAN 73 IS OBSOLETE

SECURITY CLASSIFICATION OF THIS PAGE

Unclassified

SECURITY CLASSIFICATION OF THIS PAGE(When Data Entered)

11. (Contd)

Using the Collocation and Point Mass Techniques

Unclassified

SECURITY CLASSIFICATION OF THIS PAGE(When Data Entered)

Accession For	
NTIS GRA&I	<input checked="" type="checkbox"/>
DTIC TAB	<input type="checkbox"/>
Unannounced	<input type="checkbox"/>
Justification	
By _____	
Distribution/	
Availability Codes	
Dist	Avail and/or Special
A/1	



Contents

1. INTRODUCTION	1
2. POINT-MASS APPROACH	2
3. COLLOCATION APPROACH	3
4. PRACTICAL APPLICATION OF THE COLLOCATION ALGORITHM	4
5. COMPARISON WITH THE POINT-MASS APPROACH	11
6. SUMMARY AND CONCLUSIONS	18

Illustrations

1. Global Predictions of Geoid Undulations Using Collocation With Noise Superimposed on the Spherical Harmonic (14, 14) Degree and Order Solution as Obtained From SEASAT Altimetry	7
2. Global Predictions of Gravity Anomalies Using Collocation With Noise Superimposed on the Spherical Harmonic (14, 14) Degree and Order Solution as Obtained From SEASAT Altimetry	8
3. Global Point Mass Adjustment of the Geoid Superimposed on the Spherical Harmonic (14, 14) Degree and Order Solution as Obtained From SEASAT Altimetry	9
4. Global Point Mass Predictions of Gravity Anomalies Superimposed on the Spherical Harmonic (14, 14) Degree and Order Solution as Obtained From SEASAT Altimetry	10

Illustrations

5. Rms Differences in Geoid and Gravity Anomalies Between Point Mass and Collocation Techniques in Selected Areas of Comparison	12
6. Contours of Differences of Geoid Undulations (m) Between Collocation and Point Mass Techniques, Block 4, Figure 5	13
7. Contours of Differences of Gravity Anomalies (mgal) Between Collocation and Point Mass Techniques, Block 4, Figure 5	14
8. Contours of Differences of Geoid Undulations (m) Between Collocation and Point Mass Techniques, Block 8, Figure 5	15
9. Contours of Differences of Gravity Anomalies (mgal) Between Collocation and Point Mass Techniques, Block 8, Figure 5	16

Tables

1. Results Pertained to Randomly Selected Residuals of the Collocation Approach	6
2. Differences in N and Δg Between the Two Approaches Compared	17

Global Geoid and Gravity Anomaly Predictions Using the Collocation and Point Mass Techniques

1. INTRODUCTION

The second-phase techniques, point mass and collocation with noise, allow fine structure of the earth's gravity field to be added to its long-wavelength features computed previously from satellite altimetry. The initial, or first-phase treatment of such data has been carried out at AFGL in a global short-arc adjustment of spherical-harmonic potential coefficients (typically through the degree and order 14, 14), state vector parameters and, optionally, certain tidal parameters. This adjustment has been the subject of several AFGL reports and papers, and its description will not be repeated here. The most recent reference giving sufficient information about its aspects is Reference 1.

Initially, a second-phase solution was conceived in terms of point-mass (P. M.) adjustment as the basic method for a detailed resolution of the earth's gravity field and its fundamental surface, the geoid. Due to the banded structure of the matrix of normal equations, the P. M. parameters can be resolved in overlapping strips eventually covering the whole oceanic geoid. The P. M. approach has been presented in various AFGL reports and papers, most recently in

(Received for publication 31 August 1984)

1. Blaha, G., Hadgigeorge, G., and Rooney, T. (1984) Inclusion of tidal parameters in satellite altimetry adjustment model. Paper accepted for publication in Marine Geodesy, Crane Russak, New York.

Reference 2 featuring also the results of a global adjustment. Its basic characteristics will be recapitulated here in a brief fashion.

The point-mass approach has recently been complemented by the method of least-squares collocation with noise described by Blaha,³ which provides us with another technique to recover the earth's gravity field on a local, regional or global scale. In order to achieve a detailed resolution of the gravity field, one should proceed to an evaluation of a large-scale second-phase solution in terms of both the point-mass and the collocation approach. Accordingly, this report features comparisons between these two techniques.

As has been indicated above, both second-phase approaches are based on the first-phase global adjustment of satellite altimetry. In particular, the altimeter residuals from the first phase are stored on a magnetic tape and are utilized in the second phase in the role of (new) observations. Either of the second-phase approaches accommodate the previously unmodeled effects represented by these residuals. Thus, the high-resolution altimeter information enters the second-phase adjustment.

2. POINT-MASS APPROACH

The P. M. adjustment is built on the adjusted geoid from the first phase which can represent a "normal field". The parameters in this method are the P. M. magnitudes associated with point masses distributed in an equilateral grid. The point masses can form a single layer, in which case they are all at the same depth below the surface of the reference ellipsoid. Or the point masses can form a double layer with twin point masses at each location of the grid separated by a predetermined vertical distance. The number of parameters is the same in both these modes since a twin point mass represents only one parameter; the magnitudes of the shallower and deeper point masses are equal, only their signs differ. The resolution power depends primarily on the grid interval, and to a much lesser degree on their depth and/or vertical separation of the twin point masses. This is illustrated in Table 1 of Blaha et al.² presenting results from a large test area in the southern-most portion of the Pacific Ocean. Thus, for example, if the point masses (single or twin) are distributed in a $2^\circ \times 2^\circ$ equilateral grid, the resolution corresponds very approximately to a (90, 90) spherical-harmonic expansion.

2. Blaha, G., Bessette, R. P., and Hadgigeorge, G. (1984) Global point-mass adjustment of the oceanic geoid based on satellite altimetry. Paper submitted for publication in Marine Geodesy.
3. Blaha, G. (1984) First- and Second-Phase Gravity Field Solutions Based on Satellite Altimetry. AFGL-TR-84-0083, AD A142256.

The second-phase P. M. adjustment treats the new observations, the P. M. parameters and, optionally, certain tidal parameters in a simultaneous least-squares process leading to a more detailed resolution of the earth's gravity field on the global oceanic scale.

The final outcome of the two adjustment phases with respect to the geoid and the earth's gravity field consists of a set of S. H. potential coefficients and the magnitudes of the point masses introduced at the predetermined locations, which enable one to determine geoid undulations, gravity anomalies, and so on, at any points of interest. Each such quantity is an algebraic sum of two parts, the first due to the S. H. coefficients and the second due to the P. M. parameters. The numerical values of such quantities are considered to describe the earth's gravity field to within the desired resolution.

3. COLLOCATION APPROACH

The basic difference distinguishing this approach from the P. M. adjustment, from the computational point of view, is that a simultaneous least-squares adjustment of several variables does not take place. In principle, only one prediction point is solved for at a time. Therefore, instead of an inversion of a large, strongly patterned, system of normal equations, inversions of small matrices take place. The prediction points themselves can be distributed in an equilateral grid similar (or identical) to the P. M. grid. In this case the resolution power, corresponding to an (n', n') S. H. expansion, is similar in both approaches.

The (new) observations are minus the geoidal residuals from the first phase, and they can be limited to those located within a given spherical cap from the desired prediction point. The predictions of greatest interest are those of geoid undulations, obtained through the use of the geoidal covariance function; predictions of other quantities such as gravity anomalies can be obtained for the same location upon using the appropriate cross-covariance function. All the predicted quantities refer to the "normal field" represented by an (n, n) S. H. expansion.

Since the number of observations involved with one prediction point can be made reasonably small (see, for example, weighted averaging of observations located close together as explained in Section 6.4 of Blaha,³) one is faced with inverting N small matrices as opposed to inverting an $N \times N$ system of normal equations, where N is the number of prediction points. This allows for modest computer storage requirements which are set to accommodate, in one "loop", a chosen number of prediction points together with the corresponding vectors and matrices of small dimensions. Since the prediction procedure applies to one point at a time, predictions in subsequent "loops" can be made (and stored on a

magnetic tape) for the whole oceanic geoid essentially in a grid of an arbitrarily small interval.

The predictions of the (n', n') geoid based on the (n, n) "normal field" can be made in the original equilateral grid of prediction points, rather than in a finer grid. The original grid can later be densified at will upon using the economical "errorless collocation". Such a procedure utilizes the original predictions in the role of observations.

The densified grid corresponding to the (n', n') S. H. expansion can be used for a variety of purposes. For example, it can be used for the construction of a geoidal contour map (in this case it may be useful to make it a fairly dense geographical grid). As another example, it can serve in the computation of the S. H. potential coefficients, via the integral formulas, through the degree and order (n', n') . A lower degree and order expansion, if desired, can be obtained simply by a truncation of the expansion just formulated. In a very similar procedure, the original as well as the densified grid can be made to represent other geophysical quantities besides geoid undulations, such as gravity anomalies.

4. PRACTICAL APPLICATION OF THE COLLOCATION ALGORITHM

We have already pointed out the basic, or original, predictions are considered to form an equilateral grid. Such a distribution yields a uniform resolution depending on the grid interval (the degree n' defined previously is assumed to be compatible with this interval). Accordingly, a unit sphere representing the globe is thought of as subdivided into compartments, each characterized by the appropriate angular intervals $\Delta\phi$ and $\Delta\lambda$, and each associated with one centrally located prediction point. The value of $\Delta\phi$ is independent of position, but the value of $\Delta\lambda$ varies as $\Delta\phi/\cos\phi$, where ϕ is the geocentric latitude. The poles would be an exception to this rule (the compartments would become spherical caps), but they are omitted from this development. In the case of SEASAT, for example, the ground tracks reach only the latitudes $\pm 72^\circ$ beyond which no predictions are made.

Practical considerations coupled with numerical evaluations have indicated that including observation points located within the spherical cap that just covers the corners of the compartment of the prediction point called J is reasonable. This provides for a modest measure of continuity between neighboring predictions because of the overlap in peripheral observations. The radius of such a cap, centered at J , is approximately $0.75\Delta\phi$. Even so, the number of observation points involved in one prediction may sometimes be prohibitive. This occurs in spite of the input data being limited to 0.5° -intervals along satellite arcs, and is due to a substantial increase in the number of observations brought about by the presence of

repeating tracks. It then becomes necessary to stipulate a maximum allowable number of observation points and discard the points farthest from J until this limit is satisfied. For this reason it is useful to have the observation points ordered according to their angular distances (Ψ) from J.

The global collocation results are based on the first-phase adjustment of SEASAT altimeter data carried out in terms of a (14, 14) spherical-harmonic model. The original prediction points are distributed in a $2^\circ \times 2^\circ$ equilateral grid extending over the world's oceans. This corresponds very approximately to an S. H. expansion (90, 90), hence $n' \approx 90$. The "one sigma" of the noise in the original predictions has been stipulated to be 1 m. This noise level encompasses the unaccounted for sea surface effects as well. The densification in view of contour maps (for both geoid undulations and gravity anomalies) have been made in a $1^\circ \times 1^\circ$ geographical grid using the errorless collocation technique. Residuals have been computed for 20,192 observation points selected randomly over the global ocean. The root mean square (rms) of the 20,192 residuals has been computed as 0.91 m. By comparison, the rms residual obtained through the point-mass technique has been reported in Blaha et al.² as 1.0 m.

The contour maps for N and Δg are presented in Figures 1 and 2, respectively. Their resemblance to the corresponding contour maps in the point-mass approach, Figures 3 and 4, is very satisfactory. The quantitative evaluation of this similarity will be offered in the next section. One notices somewhat irregular behavior of the contour lines not only in trench areas, but especially in areas containing a large number of islands. The latter problem is linked to altimeter errors which passed undetected through the screening process. This has been noticed mainly in the West Pacific, due to a multitude of islands some of which acted as a reflector of the radar pulse during data acquisition. For example, errors of several meters have been traced down in an area south of American Samoa. With a more elaborate screening process and, above all, with an improved distinction between the reflective surfaces (sandy beaches, and so on, vs water) expected in conjunction with future satellites, this kind of difficulty will disappear. But with the exception of the West Pacific, the SEASAT altimeter measurements appear to be reliable over the global oceanic surface.

The above discussion is illustrated and complemented with the aid of Table 1 featuring the outcome of a simple analysis of residuals. These residuals account for only a small percentage of all the available data, but they have been selected in a random fashion to adequately represent the oceanic basins. The table is self-explanatory. One notices a higher rms value (also the average magnitude) in the West Pacific, the cause of which has been mentioned in the preceding paragraph. By contrast, the East Pacific exhibits an unusually small rms residual. This ocean basin is not only void of major island clusters, but the geoidal relief is relatively

smooth. The West and East Pacific have been separated in the computation by the meridian of 205° longitude.

If both the East and West Pacific, representing the extreme values in Table 1, were left out of the computations, the results would be (in the same order):

8,971; 0.95 m 0.03 m, 0.67 m.

One notices that the contribution due to the East Pacific has had a beneficial effect on all three statistics listed in Table 1. If no ocean basin should be excluded, but the number of residuals in the East Pacific should be lowered to 4,500 so as to correspond more closely to their number in the West Pacific, the results would be

17,841; 0.95 m, 0.01 m, 0.61 m.

If the measurement errors in the West Pacific were eliminated, the rms residual would probably be brought below the 0.9 m level. But at this point the overall result can safely be presented as 0.9 m rms residual. This is about 10 percent lower than the rms residual in the point-mass approach where, however, different residual sets were used in the computation.

Table 1. Results Pertaining to Randomly Selected Residuals of the Collocation Approach

Ocean	Number of Residuals	rms Residual	Average Residual	Average Magnitude
North Atlantic	1,956	0.89 m	0.04 m	0.66 m
South Atlantic	3,987	1.01 m	0.04 m	0.69 m
Indian	3,028	0.91 m	0.00 m	0.65 m
West Pacific	4,370	1.22 m	-0.01 m	0.75 m
East Pacific	6,851	0.56 m	-0.01 m	0.37 m
Total	20,192	0.91 m	0.01 m	0.59 m

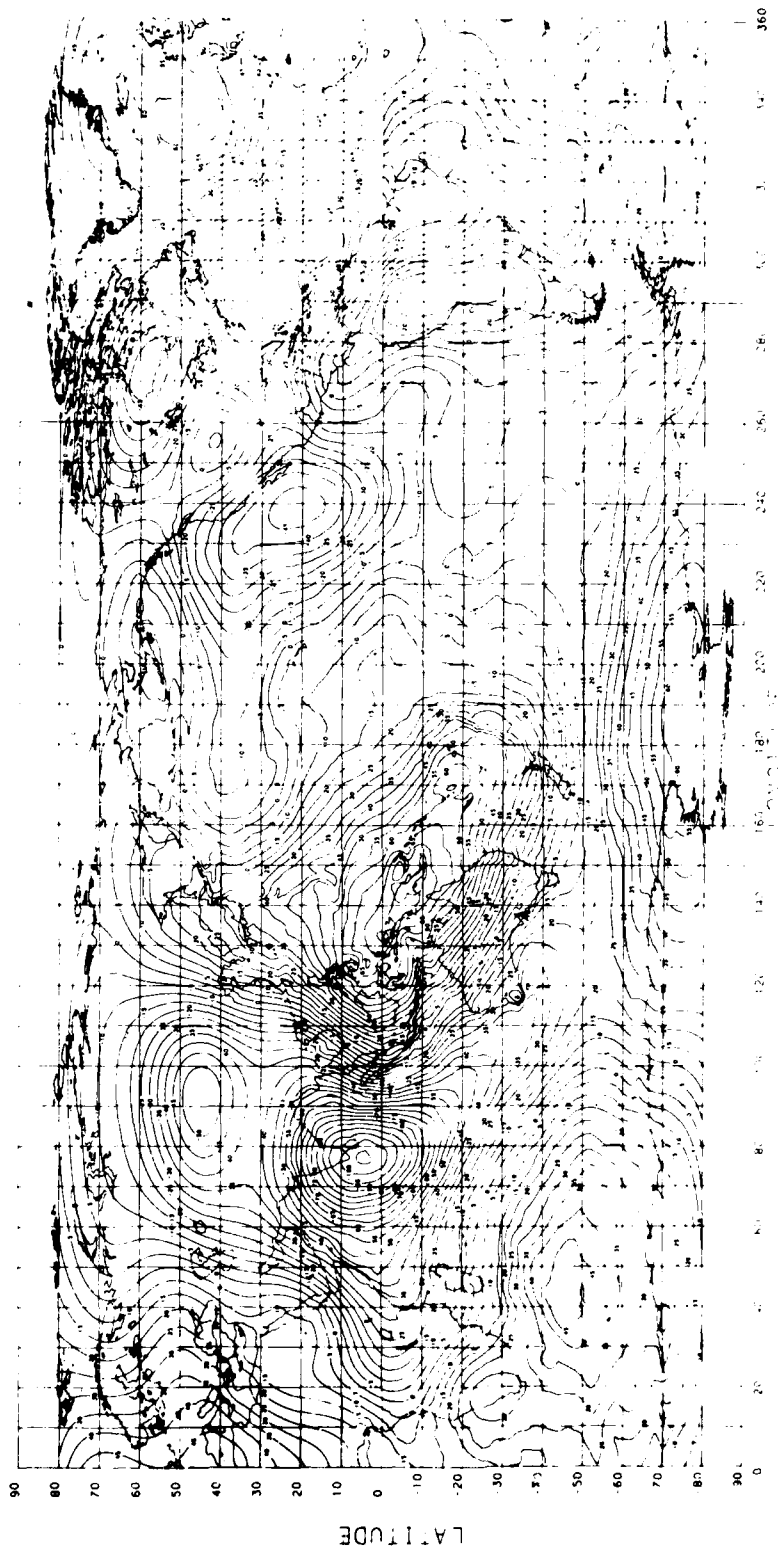


Figure 1. Global Predictions of Geoid Undulations Using Collocation With Noise Superimposed on the Spherical Harmonic (14, 14) Degree and Order Solution as Obtained From SEASAT Altimetry. Reference flattening 1/298.25, Contour Interval 5.0 m

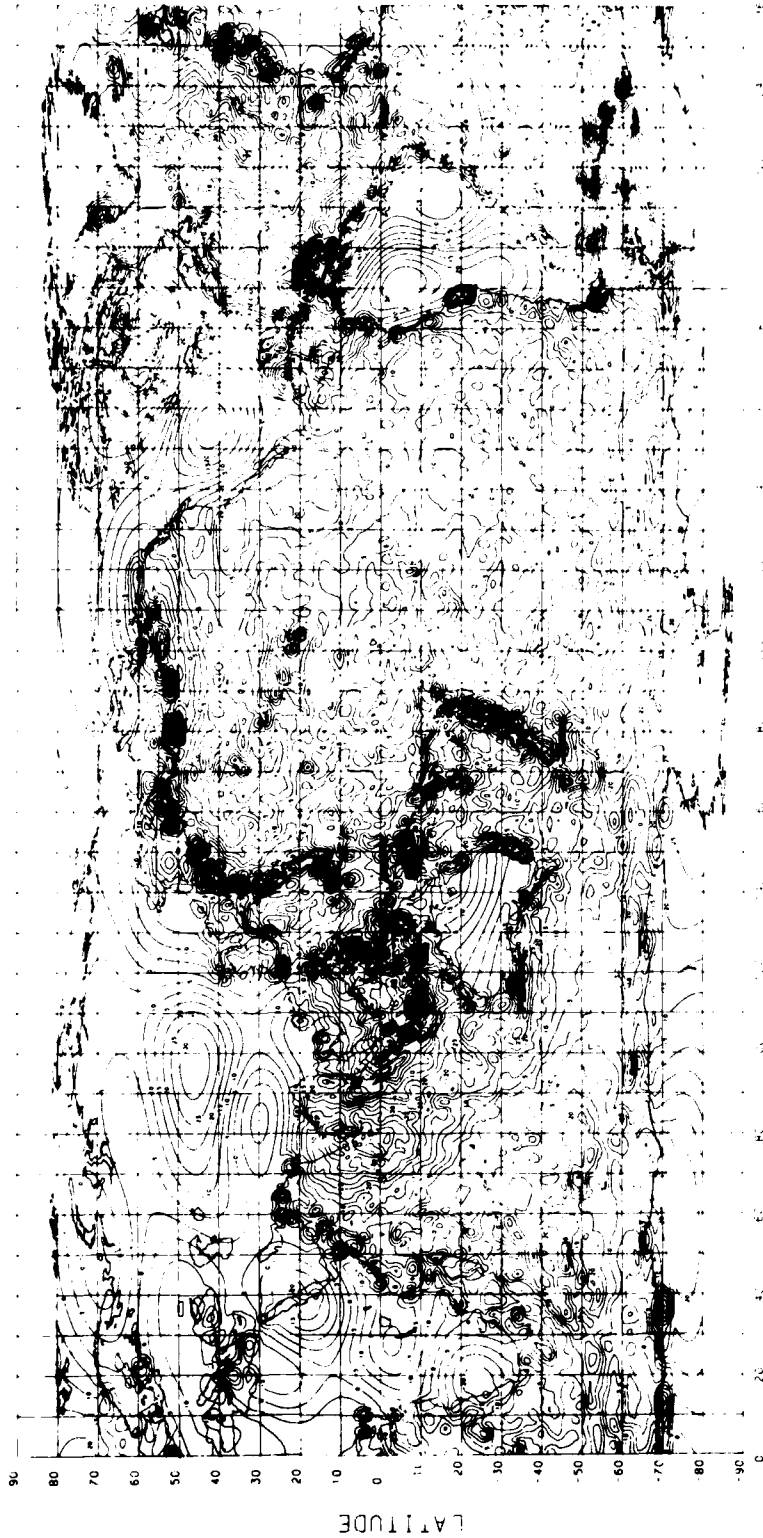


Figure 2. Global Predictions of Gravity Anomalies Using Collocation With Noise Superimposed on the Spherical Harmonic (14, 14) Degree and Order Solution as Obtained From SEASA I Altimetry. Contour Interval 5.0 mgal

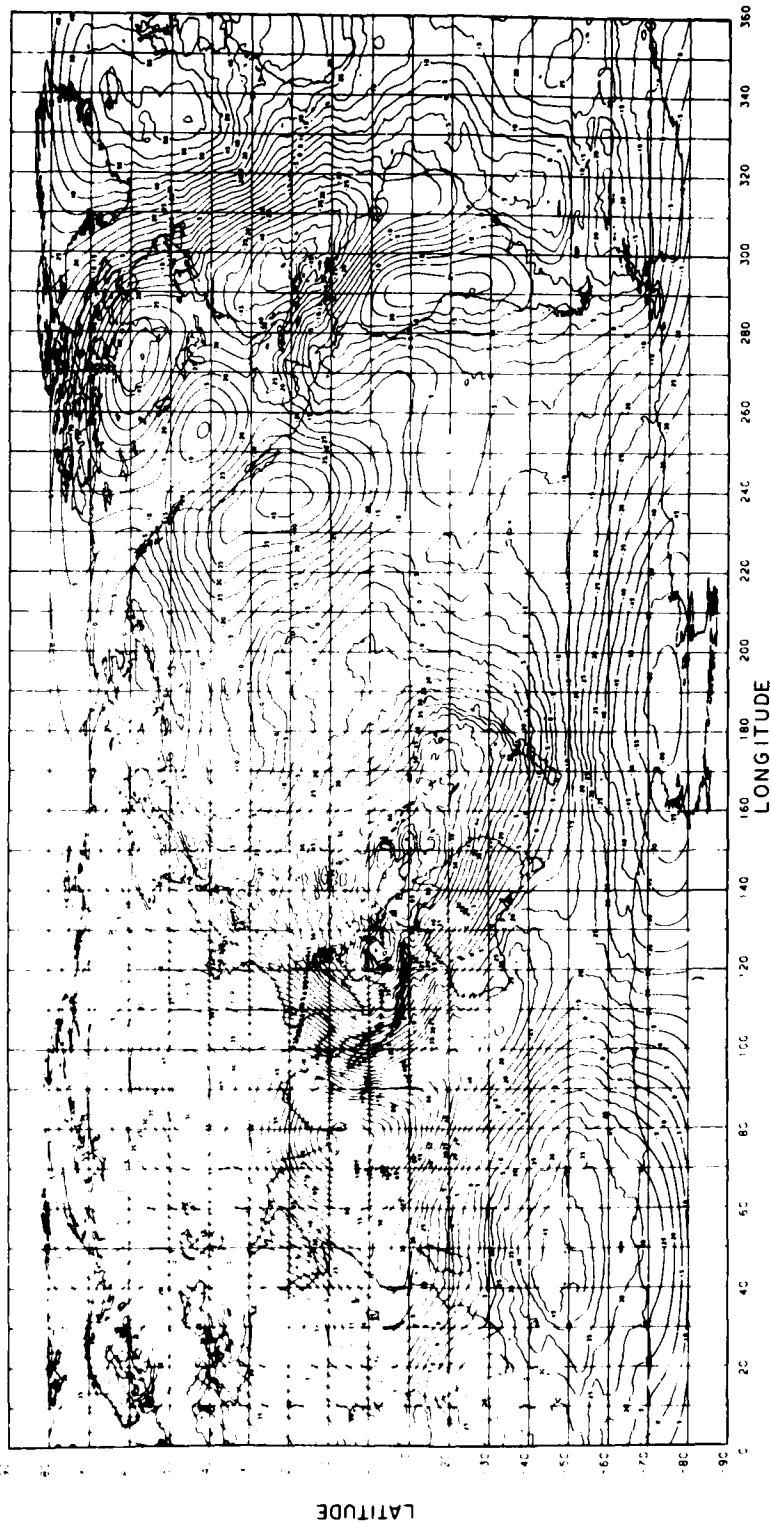


Figure 3. Global Point Mass Adjustment of the Geoid Superimposed on the Spherical Harmonic (14, 14) Degree and Order Solution as Obtained From SEASAT Altimetry. Reference Flattening 1/298.25, Contour Interval 5.0 m

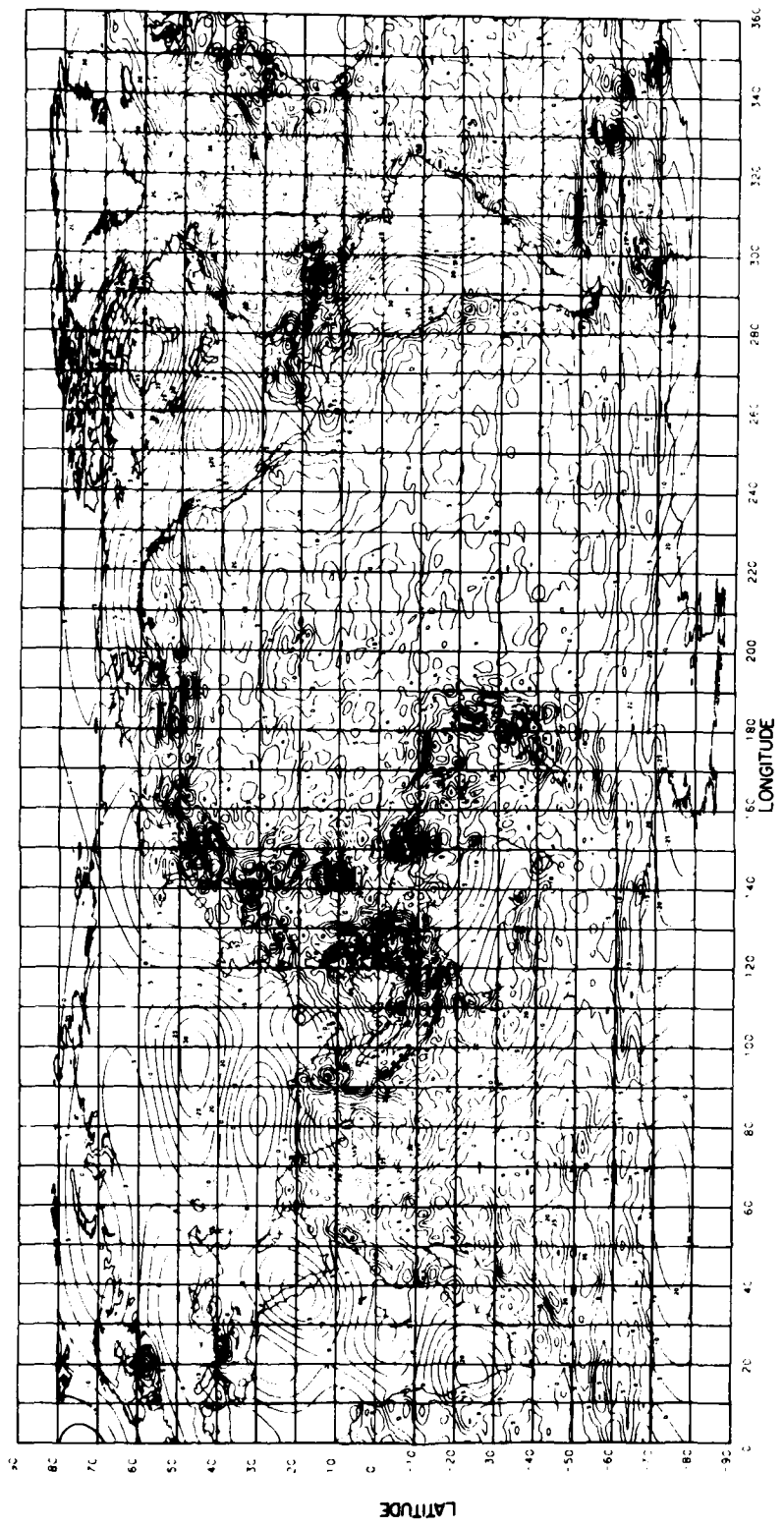


Figure 4. Global Point Mass Predictions of Gravity Anomalies Superimposed on the Spherical Harmonic (14, 14) Degree and Order Solution as Obtained From SEASAT Altimetry. Contour Interval 5.0 mgal

5. COMPARISON WITH THE POINT-MASS APPROACH

The point-mass approach and results have been presented in Blaha et al² and need not be repeated here. A casual look at the geoidal and gravity anomaly contour maps may not reveal any difference between the point-mass and the collocation technique, both applied to the same first-phase adjustment of SEASAT altimetry in terms of a (14, 14) spherical-harmonic model. A quantitative evaluation of the differences between these two techniques will follow. However, one should first realize a few basic facts.

Most importantly, a comparison is being made between two completely different and independent approaches, one based on a parameter adjustment (point-mass magnitudes) and the other based on prediction formulas using the notion of covariance (and cross-covariance) function. The locations of the original prediction points in the collocation approach are in general different from the locations of point masses in the P. M. approach, although in either case such locations form an approximate $2^\circ \times 2^\circ$ equilateral grid. However, the pertinent geophysical values are compared at the level of the densified grid, that is, the $1^\circ \times 1^\circ$ geographical grid, not at the level of the original prediction points or observation points. Thus, prediction errors due to the densification increase the uncertainty of the values actually compared; although this statement refers to the collocation approach, a similar argument can be made for the point-mass approach. The net outcome of these considerations points to a conservative nature of the comparisons. This is even more evident in the case of gravity anomalies (as opposed to geoid undulations), which can be thought of as "doubly predicted" quantities, both with regard to the function of the disturbing potential and to the location of the predictions.

The blocks of comparison between the two approaches are depicted in Figure 5. These blocks, numbered 1 through 13, cover all of the world's oceans, usually more than one block per ocean basin. The blocks have been chosen in such a way as to avoid areas containing erroneous data, especially parts of the West Pacific as discussed earlier, as well as areas of marked short-wavelength features. The latter often accompany major ocean trenches. Since the comparison concerns the 2° -resolution, features corresponding to a 1° -resolution cannot be properly represented by either method and should indeed be left out of consideration. The differences computed in the $1^\circ \times 1^\circ$ geographical grid are formed in the sense the collocation value minus the P. M. value. Figure 5 lists the rms differences for geoid undulations (in meters) and gravity anomalies (in milligals) in selected areas. Figures 6 through 9 show the contours of the differences in the above functions for the blocks numbered 4 and 8, which are judged quite representative of the overall comparison.

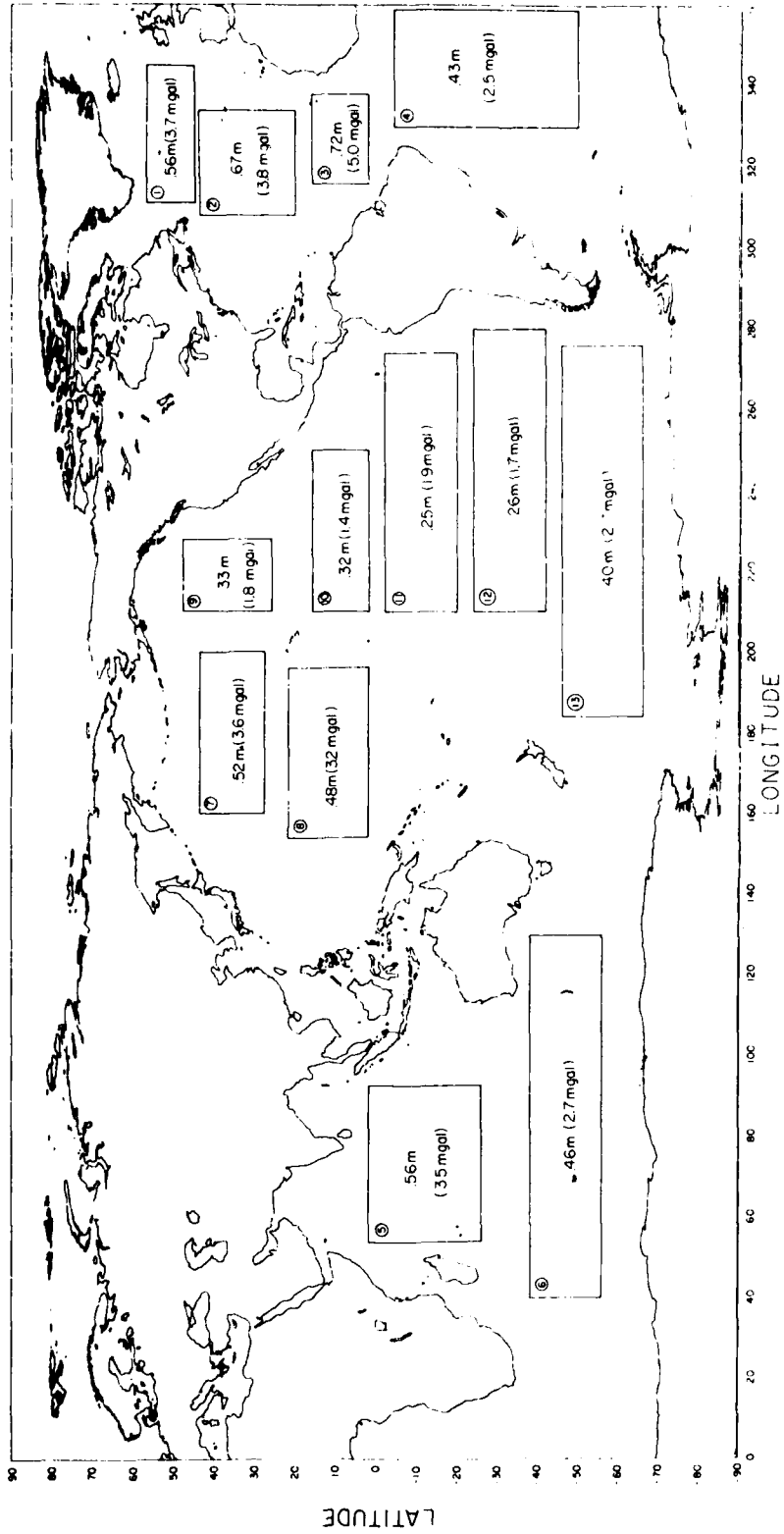


Figure 5. Rms Differences in Geoid and Gravity Anomalies Between Point Mass and Collocation Techniques in Selected Areas of Comparison

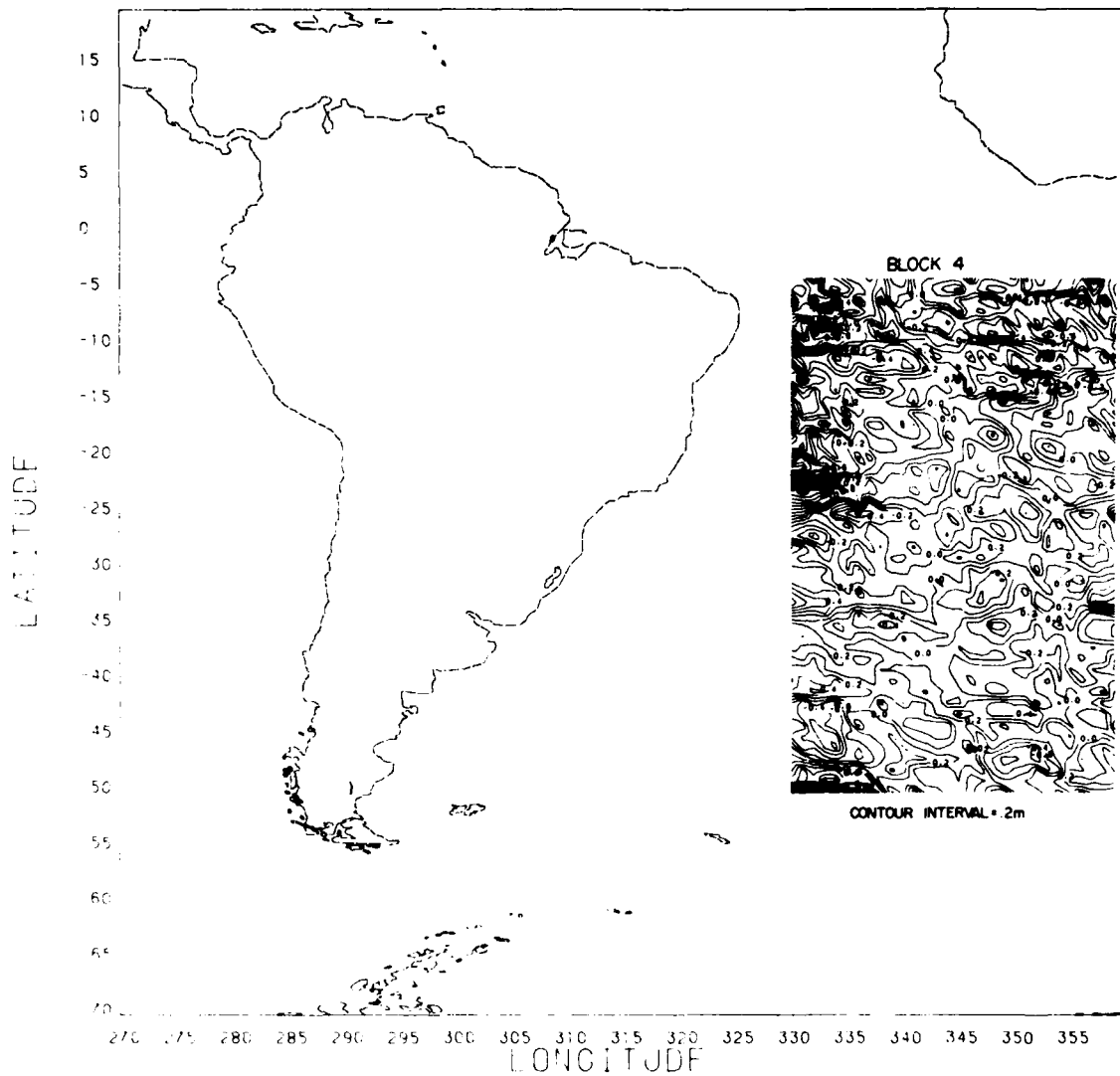


Figure 6. Contours of Differences of Geoid Undulations (m) Between Collocation and Point Mass Techniques, Block 4, Figure 5

Finally, Table 2 summarizes the numerical comparisons for all 13 blocks. Its column structure resembles Table 1, except that it contains one additional column featuring the range of the pertinent quantities (N and Δg) in each block, as estimated very approximately upon consulting Figures 1 and 2; this range thus contains the contribution of the spherical-harmonic part as well. The total rms difference is 0.45 m for geoid undulations and 2.8 mgal for gravity anomalies.

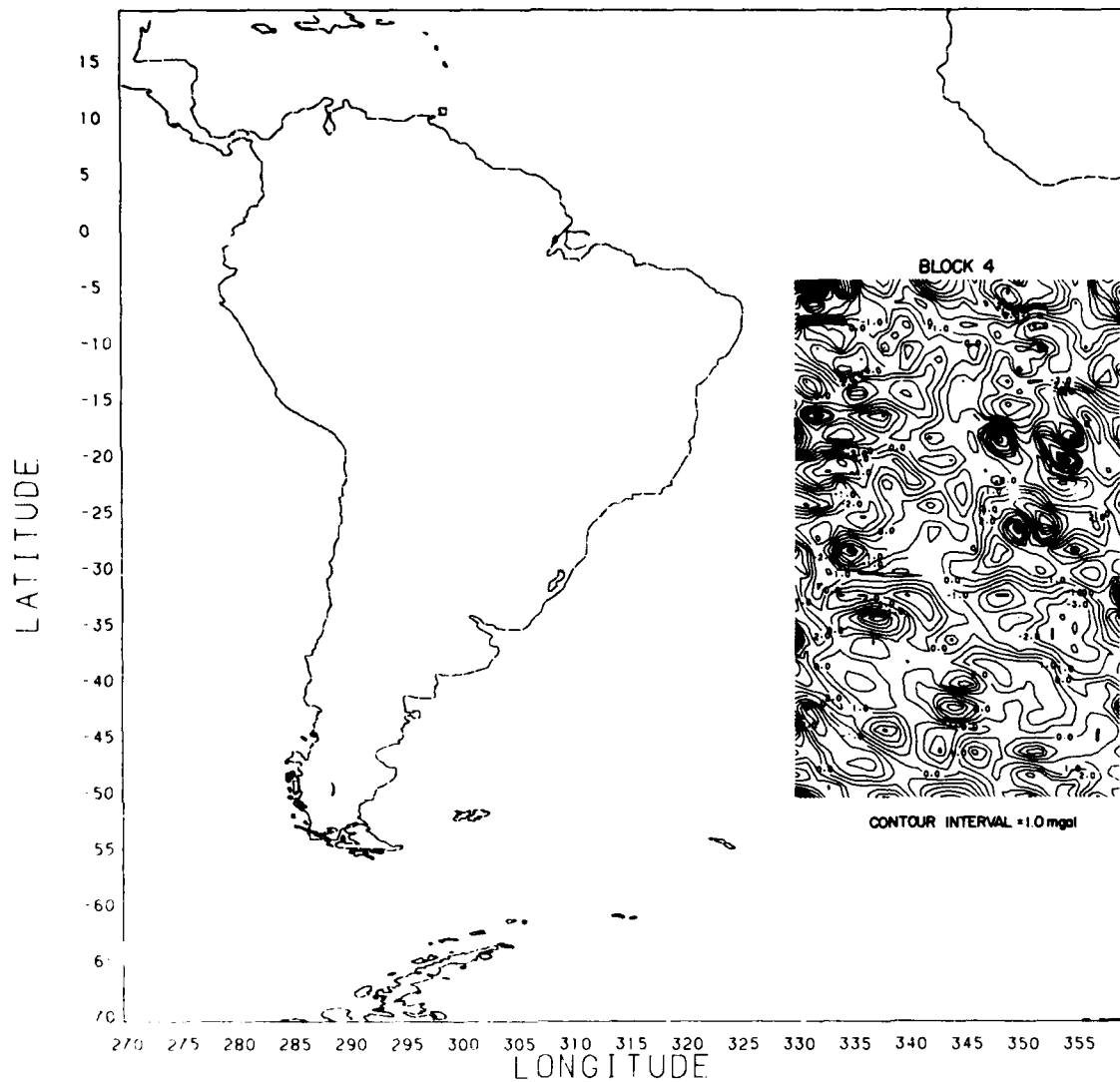


Figure 7. Contours of Differences of Gravity Anomalies (mgal) Between Collocation and Point Mass Techniques, Block 4, Figure 5

The former amounts to about 50 percent of the one sigma in the collocation approach alone, while the latter is only about 20 percent of the pertinent one sigma.

If the results of the two approaches were random with respect to each other, while each still corresponding to the 2° resolution individually, such rms differences would be expected to be on the order $\sqrt{2}$ times the appropriate sigma, that is, about 1.2 m for N and about 18 mgal for Δg . Accordingly, the compared values

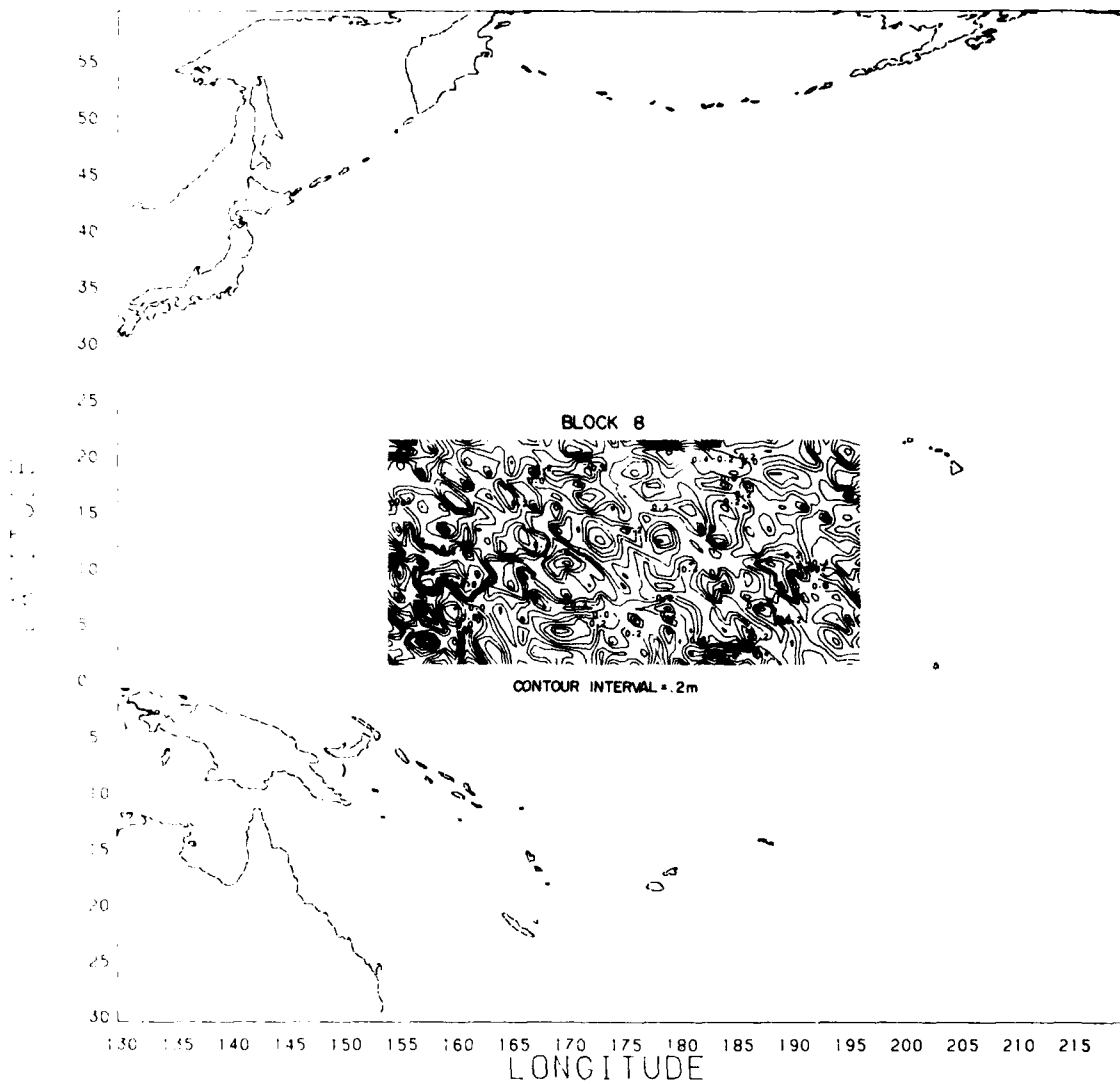


Figure 8. Contours of Differences of Geoid Undulations (m) Between Collocation and Point Mass Techniques, Block 8, Figure 5

point to an excellent agreement between the two approaches. In fact, the agreement with regard to gravity anomalies is better than expected, due perhaps to a relatively narrow range of the Δg values themselves within the blocks of comparison. One can convey the idea of similarity between the two approaches by stating that the average magnitude of the geoidal difference is merely 33 cm and the average magnitude of the gravity anomaly difference is 2.0 mgal, while the average differences are 1 cm and 0.08 mgal, respectively.

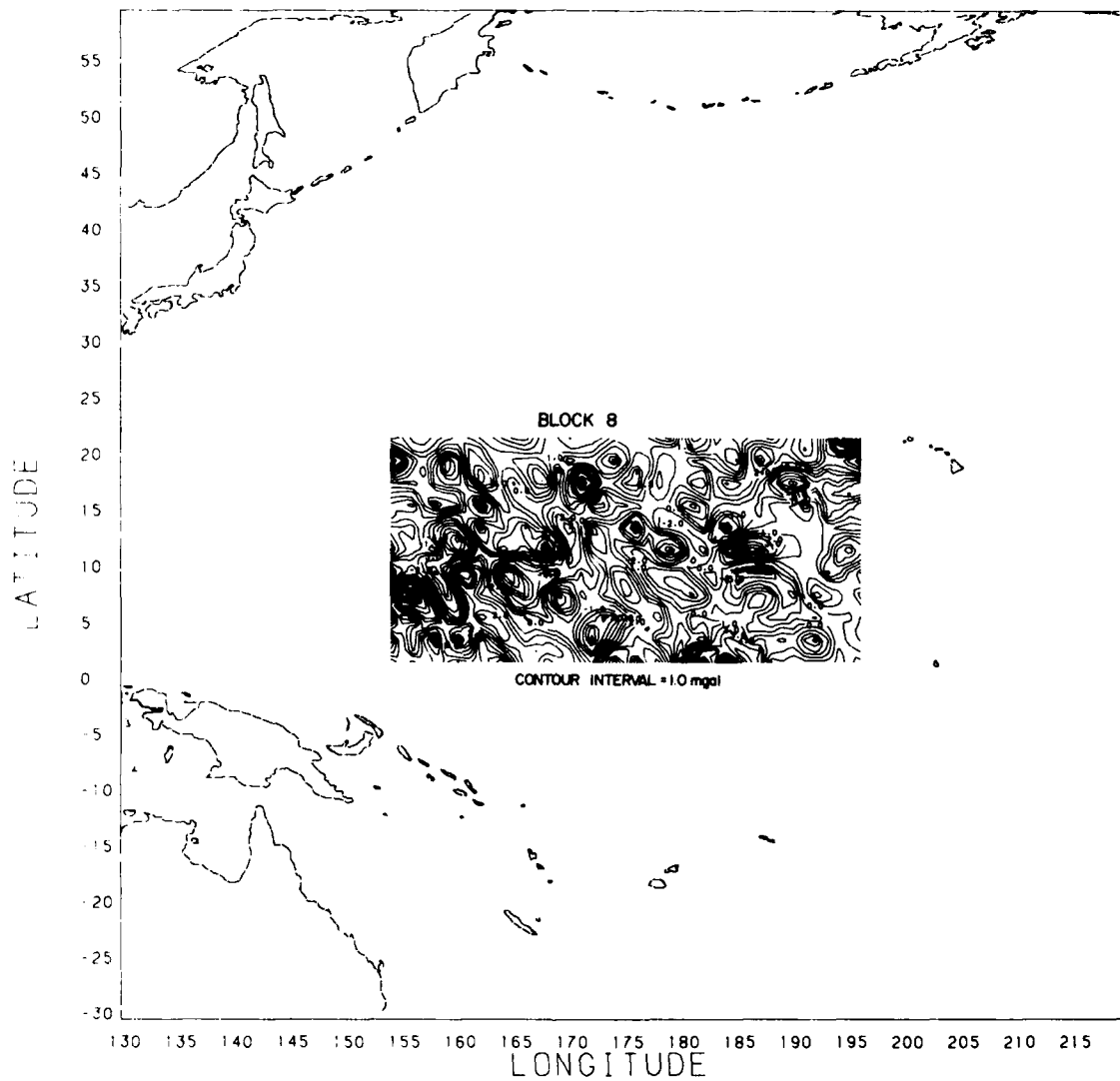


Figure 9. Contours of Differences of Gravity Anomalies (mgal) Between Collocation and Point Mass Techniques, Block 8, Figure 5

Table 2. Differences in N and Δg Between the Two Approaches Compared. The upper values correspond to N and are given in meters; the lower values (in parentheses) correspond to Δg and are given in milligals

Block	Number of Points	rms Difference	Average Difference	Average Magnitude	Range
1	455	0.56 (3.68)	-0.01 (-0.58)	0.45 (2.86)	+20, +65 (+ 5, +40)
2	675	0.68 (3.85)	-0.02 (-0.34)	0.52 (3.03)	-35, +55 (-20, +30)
3	345	0.72 (5.05)	0.01 (-0.01)	0.58 (3.57)	-35, +25 (-20, +20)
4	1,410	0.43 (2.52)	0.01 (0.10)	0.33 (1.97)	- 5, +25 (-10, +10)
5	1,131	0.56 (3.51)	0.03 (0.26)	0.43 (2.62)	-95, + 5 (-45, +10)
6	1,729	0.46 (2.68)	0.04 (0.22)	0.33 (1.96)	-35, +45 (-30, +25)
7	697	0.52 (3.61)	0.02 (-0.26)	0.40 (2.66)	-15, + 5 (-15, + 5)
8	903	0.48 (3.24)	0.02 (0.18)	0.38 (2.50)	+ 5, +55 (- 5, +10)
9	437	0.33 (1.80)	-0.02 (-0.17)	0.24 (1.37)	-40, -10 (-20, + 5)
10	615	0.32 (1.36)	-0.03 (-0.52)	0.23 (1.04)	-45, +10 (-20, +10)
11	1,235	0.25 (1.94)	0.00 (0.14)	0.19 (1.39)	-20, +15 (-10, +10)
12	1,349	0.26 (1.73)	0.01 (0.18)	0.20 (1.34)	-10, +10 (-10, + 5)
13	1,953	0.40 (2.68)	0.01 (0.21)	0.30 (2.03)	-55, 0 (-20, +10)
Total	12,934	0.45 (2.84)	0.01 (0.08)	0.33 (2.05)	-95, +65 (-45, +40)

6. SUMMARY AND CONCLUSIONS

The global first-phase adjustment of satellite altimetry described in Blaha et al¹ is a basis for a more detailed second-phase treatment of altimeter information via the point-mass and collocation techniques. Both of the second-phase techniques allow the short-wavelength detail to be added to the long-wavelength features of the earth's gravity field as expressed via spherical-harmonic potential coefficients from the first-phase adjustment. Also both approaches emphasize the determination of the oceanic geoid which is directly related (except for sea surface effects) to the altimeter measurements. The desired gravity field detail described in this report corresponds to a 2°-resolution, approximately equivalent to a (90, 90) spherical-harmonic expansion. A brief summary of the treatment of altimeter data including the comparison between the two approaches follows.

- The point-mass adjustment has proceeded in a single-layer mode; its main outcome (geoid undulation and gravity anomaly contour maps) is presented in Figures 3 and 4.
- This mode is more economical than the double-layer mode, yet the resolution power is comparable.²
- The rms residual from the point-mass adjustment has been reported as 1.0 m, which corresponds very well to the theoretical sigma characterizing the (90, 90) truncation of the spherical-harmonic mode.
- The smoothed out predictions of geoid undulations and gravity anomalies in the collocation approach are obtained in a 2° × 2° equilateral grid with the aid of the modified collocation with noise technique.
- The densification of this grid is carried out by means of the errorless collocation, resulting in a 1° × 1° geographical grid suitable for the construction of geoid undulation and gravity anomaly contour maps.
- The residuals in the collocation approach are computed via the errorless collocation; this process is compatible with the construction of the geoidal contour map.
- The rms residual from a random sample of 20, 192 residuals from collocation approach is computed as 0.91 m, which accords very well with the truncation of an equivalent spherical-harmonic model, with the rms residual of the point-mass approach, and with the one sigma associated with the geoidal contour map.
- The average residual is similarly computed as 1 cm and the average magnitude of the residuals is computed as 59 cm.
- The comparison of results for both N and Δg values proceeds in 13 blocks depicted in Figure 5, encompassing 12, 934 grid points.

- The rms difference in N between the two techniques is computed as 0.45 m; the rms difference in Δg is 2.8 mgal.
- The average difference in N is 1 cm, while it is 0.08 mgal for Δg ; the average magnitudes of the differences are 33 cm and 2.0 mgal, respectively.
- The geoidal and gravity anomaly results from the two approaches are thus seen to correspond very closely to each other. It can be concluded that these techniques confirm and verify each other.

END

FILMED

7-85

DTIC